Dynamics of an Elementary Bond-Forming Process: Associative Ionization in H(1s) + H(2s) Collisions

X. Urbain, A. Cornet, and F. Brouillard

Département de Physique, Unité de Physique Atomique et Moléculaire, Université Catholique de Louvain, Chemin du Cyclotron 2, B 1348 Louvain-la-Neuve, Belgium

A. Giusti-Suzor[a]

Laboratoire de Chimie Physique, Université de Paris VI, rue Pierre et Marie Curie 11, F 75005 Paris, France

(Received 22 October 1990)

Using a merged-beam apparatus, we have measured the absolute cross section for the associative ionization process $H(1s)+H(2s)\rightarrow H_2^+ e^-$ between 0.5 and 10 eV. The total cross section rises until a maximum of 2.4×10^{-17} cm^2 at the H_2^+ dissociation threshold (3.4 eV) and exhibits a minimum around 2 eV. We attribute this feature to interferences between two reaction paths. Calculations combining a quantum-defect treatment of the multichannel ionization with a close-coupling treatment of the atom-atom half collision yield results in good agreement with experiment.

PACS numbers: 34.50.Lf, 82.30.Nr, 82.40.Dm

Associative ionization (AI) is the most elementary collisional process to form molecular bonds. The net result of an AI reaction is the transfer of the translational energy of the colliding atoms into kinetic energy of the departing electron. Considering the reduced-mass ratio between the entrance and exit particles, it is clear that this energy transfer must proceed through short-range Coulomb and exchange interactions, resulting in a complete rearrangement of the electronic clouds. Associative ionization therefore provides a simple inelastic process to investigate fundamental aspects of chemical reactivity and bound-free transitions in atomic collisions.[1]

We have previously investigated the ionic case $H^+ + H^-$, both experimentally[2] and theoretically.[3] This highly exothermic reaction is dominated by the Coulombic attraction, and therefore allows little insight into the details of the reaction mechanisms. Here we consider the simplest case of neutral H+H* collisions, i.e., H(1s) +H(2s), that involves a minimal number of molecular potential curves with a threshold at 0.75 eV. Molecular data extracted from a combination of different types of calculations and spectroscopic observations are available and are used here in a careful quantal treatment of the dynamics. On the other hand, we have performed absolute measurements of the cross section that cover the whole energy domain where the AI reaction is significant. From the comparison between experimental and theoretical results, we think we have reached a thorough understanding of the main aspects of this elementary reaction.

The experimental setup (Fig. 1) is an improved version of the merged-beam single-source apparatus previously used to study ion pair production in H(1s)+H(2s) collisions.[4]

An intense 6.5-keV hydrogen beam is extracted from a discharge source in the focalizing field of a twin extractor. The initial compression of the beam is maintained by the strongly focusing lens preceding the mass analysis. The protons are separated from the major H_2^+ and H_3^+ components in a 45° magnetic sector, the conical pole pieces of which ensure a stigmatic focusing. The resulting proton beam is then decelerated down to 2 keV inside a lens doublet. The whole transportation line (from the extractor to the decelerator) is electrically fed with respect to the source potential, and is therefore independent of the actual acceleration voltage. This feature allows us to sweep the proton energy without disturbing the primary focusing and mass selection.

Excited hydrogen atoms are obtained from electron capture by protons on cesium, a resonant process leading to the different $n=2$ states. The major $2p$ fraction quickly decays to the ground state. Electric-field calculations indicate that the metastable $2s$ fraction, 25% of 2 keV,[5] is quenched to 15% before the interaction region is reached. A pure H(1s) beam is produced upstream by charge exchange in a xenon cell. The neutral beams are

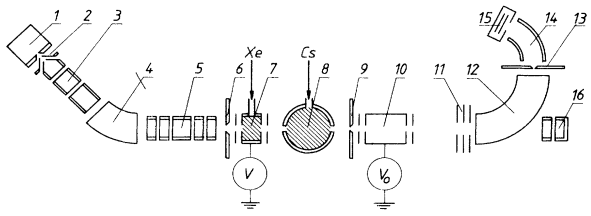

FIG. 1. Experimental setup: (1) duoplasmatron source, (2) twin extractor, (3) electrostatic lens, (4) magnetic sector, (5) lens doublet, (6) 3-mm-diam aperture, (7) xenon cell (bias voltage V), (8) cesium oven, (9) 1-mm-diam aperture, (10) observation cell (bias voltage V_0), (11) three-aperature lens, (12) magnetic sector, (13) slit, (14) cylindrical deflector, (15) ion detector, and (16) secondary-emission probe.

given a velocity difference by applying a bias voltage on this first cell. The geometry of the merged beams is determined by two diaphragms located on either side of the neutralization stage. Under these conditions, neutral-atom fluxes of the order of 5×10^{14} cm^{-2}s^{-1} have been achieved in both beams, providing an unprecedented luminosity in fast merged-beam experiments.

The interaction length is defined, as previously, by means of an observation voltage applied on a gridded box surrounding the beam. This voltage determines the kinetic energy of the H_2^+ ions, so that these can be separated, in the subsequent energy analysis, from ions produced elsewhere. This is performed by a 90° magnetic sector followed by a narrow slit. The ions are detected on a Johnston mesh multiplier, behind an additional 60° cylindrical electrostatic deflector that screens it against the important flux of UV photons produced by the complete quenching of the H(2s) inside a three-aperture lens preceding the analyzer. The detection efficiency has been determined by controlled attenuation of a 4-keV H_2^+ beam.

The flux of neutral atoms is measured downstream, using a negatively biased copper probe coupled to a fast electrometer. Its secondary-emission coefficient for atomic-hydrogen impact has been assumed to be 1.15 times that measured for protons.[6]

Absolute values of the total cross section have been obtained[7] between 0.5 and 10 eV by repeated sweep of the relative velocity of the reactants. The kinetic energy of the outgoing H_2^+ was kept constant by synchronously varying the proton acceleration voltage and the xenon-cell bias voltage. A detailed description of the experimental method will be published elsewhere. The experimental values are shown in Fig. 2. Error bars represent the standard deviation of the ion yield. Errors in the determination of the metastable fraction, detection efficiency, and neutral fluxes amount to a 20% uncertainty on the absolute size of the cross section.

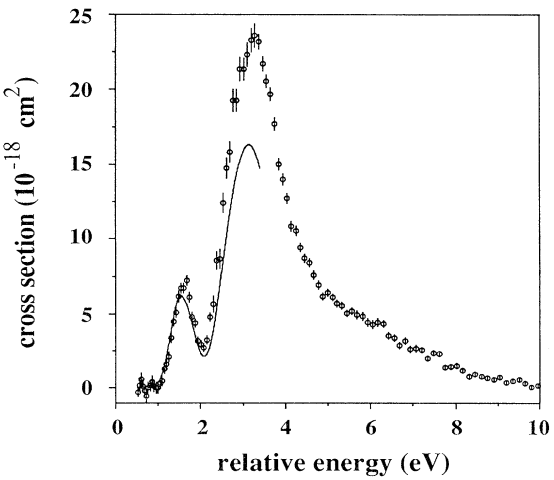

FIG. 2. Total cross section for the reaction H(1s)+H(2s) $\rightarrow H_2^+ + e^-$. The theoretical results (solid line) have been convoluted with the experimental energy resolution.

A theoretical study of the AI process measured above has been performed[7] and will be described at length in a forthcoming publication. Here we analyze the basic mechanisms for the ion formation, from which a qualitative understanding of the experimental features can already be obtained. We then outline the main points of the treatment and present numerical results.

Even for such a simple system as H+H*, the theory of AI must account for several features.

(i) Two types of continua—electronic and nuclear—are involved simultaneously. The whole process may be viewed as a *reactive* collision involving two arrangements: atom-atom (entrance associative channels) and electron-molecular ion (outgoing ionization channels).

(ii) Several types of interactions couple the different channels. Among the electron-ion channels, *vibrational* interactions couple Rydberg and/or continuum states with the same ion core but different vibrational wave functions. *Dielectronic* interactions couple this set of singly excited states with the core-excited dissociative states. Finally, the atom-atom channels experience additional couplings at long range, on their way to dissociation.

(iii) Two reaction mechanisms coexist and can interfere: the *direct* electronic autoionization of a doubly excited molecular state, and the *indirect* formation of molecular ions via vibrational autoionization of excited Rydberg levels. These levels are temporarily formed through electronic coupling with a neutral doubly excited state and induce resonances in the total cross section.

The overall energy behavior observed for the cross section may be roughly understood from examination of the main potential curves involved in the process [Fig. 3(a)]. The ion formation is mainly due to electronic autoionization of the doubly excited state (labeled 2) and the reaction probability increases with energy above the reaction threshold for $H_2^+(v=0,N=0)$ as new rovibrational levels open for ionization. When the ion dissociation limit (3.4 eV) is reached, the cross section begins to decrease [Fig. 3(b)] due to competition with dissociative ionization into $H+H^++e^-$.

However, these basic mechanisms do not explain the local minimum exhibited by the cross section around 2 eV. The separated-atom limit consists of the two almost degenerate H(1s)+H(2s,2p) combinations. Nonadiabatic transitions occur between these channels[8] when they transform into the hybrids H(2$s\pm2p$) [region P in Fig. 3(a)]. The adiabatic energies then split apart due to the avoided crossing with the ionic H^++H^- channel. At shorter internuclear distances, the two states get a dominant singly or doubly excited character, respectively, and the transitions around region Q are now governed

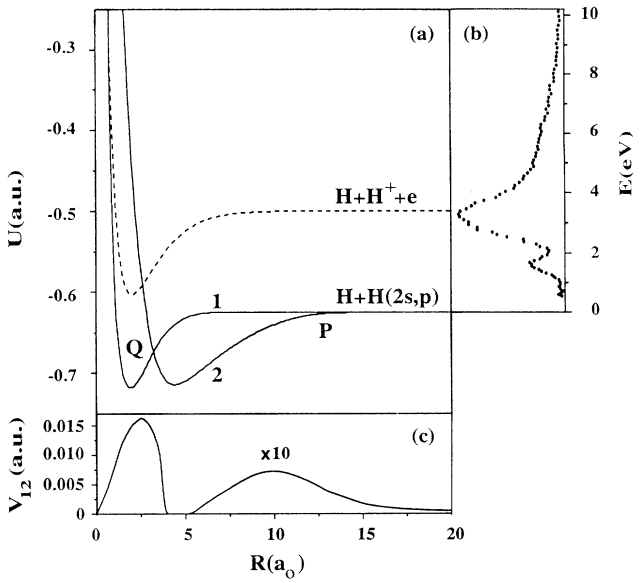

FIG. 3. Dynamics of the process. (a) Diabatic curves from Ref. 16: curve 1, $1s\sigma_g 2s\sigma_g$; curve 2, $2p\sigma_u 2p\sigma_u$. P and Q are transition regions. (b) Measured cross section. Calculated electronic coupling ($\times 10$ between $5a_0$ and $20a_0$).

by dielectronic interaction. The probability amplitudes developing independently along paths 1 and 2 [Fig. 3(a)] interfere when resumming at the inner crossing point and cause the oscillatory behavior observed in the cross section. As pointed out by Rosenthal for $He^+ + He$ collisions,[9] the two transition regions allow the interference to show up in the total cross section with a *single passage* of the collision partners.

The actual calculations use a two-step version of the multichannel quantum-defect theory (MQDT),[10] extended here to include a quantitative treatment of the atom-atom multichannel half collision. In a preliminary step, the channels corresponding to the electron-ion arrangement, on one hand, and to the atom-atom arrangement, on the other hand, are treated independently. The first set consists of ionization channels defined by the l partial wave of the external electron outside the ion core, and by their thresholds which are the successive rovibrational levels of the ion ground state. For each value of l and λ (projection onto the molecular axis) the quantum-defect function $\mu_{l\lambda}(R)$ is sufficient to account for the interchannel vibrational coupling, through the mixing coefficients

$$\mathcal{C}^N_{vv'} = \int \chi^N_v(R)\cos[\pi\mu_{l\lambda}(R)]\chi^N_{v'}(R)dR\,,$$
$$\mathcal{S}^N_{vv'} = \int \chi^N_v(R)\sin[\pi\mu_{l\lambda}(R)]\chi^N_{v'}(R)dR\,, \quad (1)$$

where χ^N_v is the vibrational wave function for the ion rovibrational level (v,N). We assume the rotational quantum number N to be conserved for each collision, thus neglecting any rotational coupling. Following the MQDT approach,[11] we treat open and closed channels identically at this stage.

The second set of channels consists of the entrance channel and the molecular states coupled to it at large distance. Using the *close-coupling* method, we solve the system of coupled radial equations for the *full* collision and extract the corresponding reactance matrix $K_{dd'}$ from the asymptotic forms of the channel wave functions

$$\Psi^N_d(q,R) = \sum_{d'} \Phi_{d'}(q,R)F^N_{d'd}(R)\,, \quad (2)$$

where Φ_d are the Born-Oppenheimer electronic wave functions of the molecular states and q stands for the electronic coordinates. We also obtain the matrix of radial solutions $F^N_{dd'}(R)$ with proper normalization, to be used in the next step of the treatment, which accounts for the interaction between the two types of arrangements.

The basic quantities for this step are the dielectronic couplings $V^{l\lambda}_d(R)$ between a given Rydberg configuration (external orbital $l\lambda$) and the doubly excited component of each dissociative state d. The corresponding interaction matrix elements

$$V^{Nl\lambda}_{vd} = \sum_{d'} \int \chi^N_v(R)V^{l\lambda}_{d'}(R)F^N_{d'd}(R)dR \quad (3)$$

form the off-diagonal blocks between the two sets of channels (ionization and dissociation). This interaction matrix is identified with the partial reactance matrix K_{vd} associated with the electronic part of the total Hamiltonian. This treatment is thus essentially equivalent to the multichannel distorted-wave Born approach developed for reactive scattering.[12] Whenever a new dissociation threshold $H + H(n \geq 3)$ is reached, one more dissociative channel is introduced with matrix elements $K_{dd'}$ calculated at first order. We then combine the K_{vd} and $K_{dd'}$ matrix elements with the set of vibrational mixing coefficients and build a generalized scattering matrix involving the total number of channels. Finally, this matrix is contracted[11] to yield the physically relevant scattering matrix S restricted to open channels. The total cross section for associative ionization is obtained through a partial-wave and vibrational summation of matrix elements $|S^N_{vd}|^2$. The partial waves of a given parity are weighted according to the prescriptions of nuclear-spin statistics.[13]

Among the four molecular symmetries correlated with the $H(1s) + H(n=2)$ limit, the $^1\Sigma_g^+$ and $^3\Sigma_u^+$ ones lead to doubly excited diabatic states at short range.[7] However, we disregard the triplet symmetry because the $(2p\sigma_u 3s\sigma_g)\,^3\Sigma_u^+$ configuration state has a very small autoionization width and lies way up in the ionization region. The relevant $^1\Sigma_g^+$ states are the $1s\sigma_g 2s\sigma_g$ Rydberg state and the first core-excited state $(2p\sigma_u)^2$ [curves 1 and 2 in Fig. 3(a)]. The large autoionization width of the latter is known both from electron-ion scattering cal-

culations[14] and from deperturbation of *ab initio* adiabatic curves.[15] The diabatic quantum defects $\mu_{s\sigma}(R)$ and $\mu_{d\sigma}(R)$ are taken from the global MQDT deperturbation of the adiabatic curves performed by Ross and Jungen.[16] The corresponding diabatic curves, connected at larger distances with the adiabatic ones, are used in the close-coupling calculation for the atomic half collision. This step also involves the long-range interaction between the asymptotic $H(1s)+H(2s,2p)$ channels. As suggested by Beswick and Glass-Maujean,[17] this nonadiabatic radial coupling, known from *ab initio* calculations,[18] has been transformed, through an R-dependent 2-by-2 rotation, into the potential-like coupling function shown in the right-hand part of Fig. 3(c). Note that this transformation does not alter the short-range diabatic picture since the two transition regions do not overlap.

The results are reported in Fig. 2 together with the experimental values. The absolute value of the cross section, in good agreement with experiment, is roughly twice as large as the theoretical results of Takagi and Nakamura,[19] who divided their results by a factor of 2, which comes from a different interpretation of nuclear-spin statistics. In the high-energy range, the discrepancy between theory and experiment probably originates in our first-order treatment of the ionization loss due to the $H+H(n\geq 3)$ escape channels. We plan to account more properly for this competition by including these additional channels in the close-coupling treatment.

Most satisfying is that the interference pattern analyzed above is well produced when the close-coupling calculation for the entrance half collision is combined with the MQDT treatment. A similar interference effect has been recently demonstrated for the $H(2p)$ to $H(2s)$ branching ratio in the photodissociation of molecular hydrogen.[20]

For the energy range of pure associative ionization (below 3.4 eV), we think that the present calculations do account for the most important features in the dynamics of this AI process. The strong interference effect demonstrated by the experimental results emphasizes the need for a detailed multichannel treatment in each particle arrangement. The theoretical approach reported here could be applied to the interpretation of polarization-sensitive experiments like $Na(3P)+Na(3P)$ associative ionization, and to the calculation of branching ratios in the dissociative recombination of molecular ions.

The authors warmly thank J. Baudon, P. Defrance, and F. H. Mies for very stimulating discussions, and S. Ross and Ch. Jungen for providing them with numerical data. This work has been supported by the Belgian Fonds National de la Recherche Scientifique (FNRS) and partly by an international collaborative NATO grant. X.U. is Chargé de Recherches FNRS.

---

[a]Also at Laboratoire de Photophysique Moléculaire, Université Paris-Sud, F 91405 Orsay, France.

[1]J. Weiner, F. Masnou-Seeuws, and A. Giusti-Suzor, Adv. At. Mol. Opt. Phys. **26**, 211 (1990).

[2]G. Poulaert, F. Brouillard, W. Claeys, J. W. McGowan, and G. Van Wassenhove, J. Phys. B **11**, L671 (1978).

[3]X. Urbain, A. Giusti-Suzor, D. Fussen, and C. Kubach, J. Phys. B **19**, L273 (1986).

[4]D. Fussen, W. Claeys, A. Cornet, J. Jureta, and P. Defrance, J. Phys. B **15**, L715 (1982).

[5]Vu Ngoc Tuan, G. Gautherin, and A. S. Schlachter, Phys. Rev. A **9**, 1242 (1974).

[6]J. A. Ray, C. F. Barnett, and B. Van Zyl, J. Appl. Phys. **50**, 6516 (1979).

[7]X. Urbain, thesis, Université Catholique de Louvain, 1990 (unpublished).

[8]J. T. Lewis, Proc. Phys. Soc. A **68**, 632 (1955); V. Sidis, C. Kubach, and D. Fussen, Phys. Rev. A **27**, 2431 (1983).

[9]H. Rosenthal, Phys. Rev. A **4**, 1030 (1971).

[10]A. Giusti, J. Phys. B **13**, 3867 (1980).

[11]M. J. Seaton, Rep. Prog. Phys. **46**, 167 (1983).

[12]W. H. Miller, J. Chem. Phys. **50**, 407 (1969); L. M. Hubbard, S. Shi, and W. H. Miller, J. Chem. Phys. **78**, 2381 (1983).

[13]J. S. Cohen, Phys. Rev. A **13**, 99 (1976).

[14]J. Tennyson and C. J. Noble, J. Phys. B **18**, 155 (1985), and references therein.

[15]L. Wolniewicz and K. Dressler, J. Chem. Phys. **82**, 3292 (1985).

[16]S. Ross and Ch. Jungen, Phys. Rev. Lett. **59**, 1297 (1987).

[17]J. A. Beswick and M. Glass-Maujean, Phys. Rev. A **35**, 3339 (1987).

[18]F. Borondo, A. Macias, and A. Riera, Chem. Phys. **81**, 303 (1983).

[19]H. Takagi and H. Nakamura, J. Chem. Phys. **88**, 4552 (1988).

[20]M. Glass-Maujean, H. Frohlich, and J. A. Beswick, Phys. Rev. Lett. **61**, 157 (1988).